Electronic Supplementary Material (ESI) for Journal of Materials Chemistry B.

Supporting information

Molecular Engineering to Enhance the Reactive Oxygen Species Generation of AIEgens and Exploration of Their Versatile Applications

Weidong Yin,[a] Jianqing Li,[b] Yucheng Ma,[a] Longjiang Xing,[a] Zeduan Chen,[a] Bo Liu,[a] Yanping Huo,[a] Zujin Zhao,*[b] and Shaomin Ji*[a]

Light Industry and Chemical Engineering College, Guangdong University of Technology, Guangzhou, Guangdong 510006, China

E-mail: smji@gdut.edu.cn

Contents

1. Experimental details

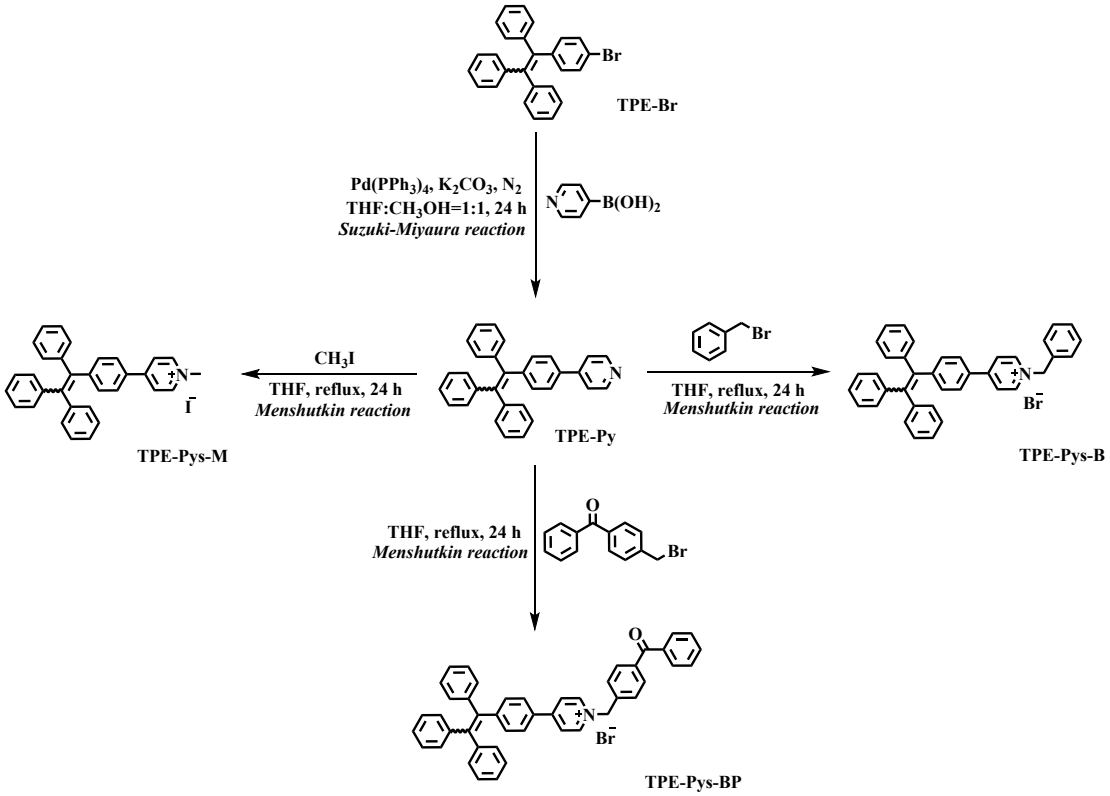

Scheme S1. Synthetic routes of TPE-Py, TPE-Pys-M, TPE-Pys-B and TPE-Pys-BP.

2. ^{1}H NMR and ^{13}C NMR Spectra of compounds

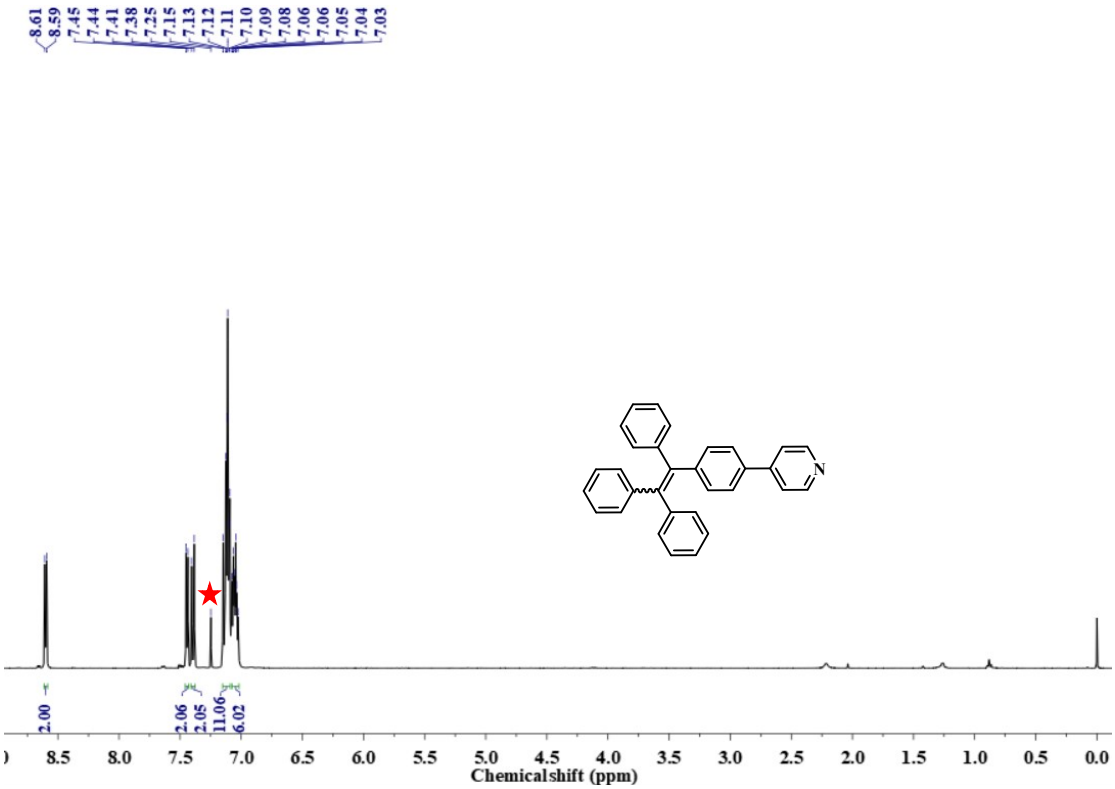

Figure S1. ^{1}H NMR Spectra of TPE-Py.

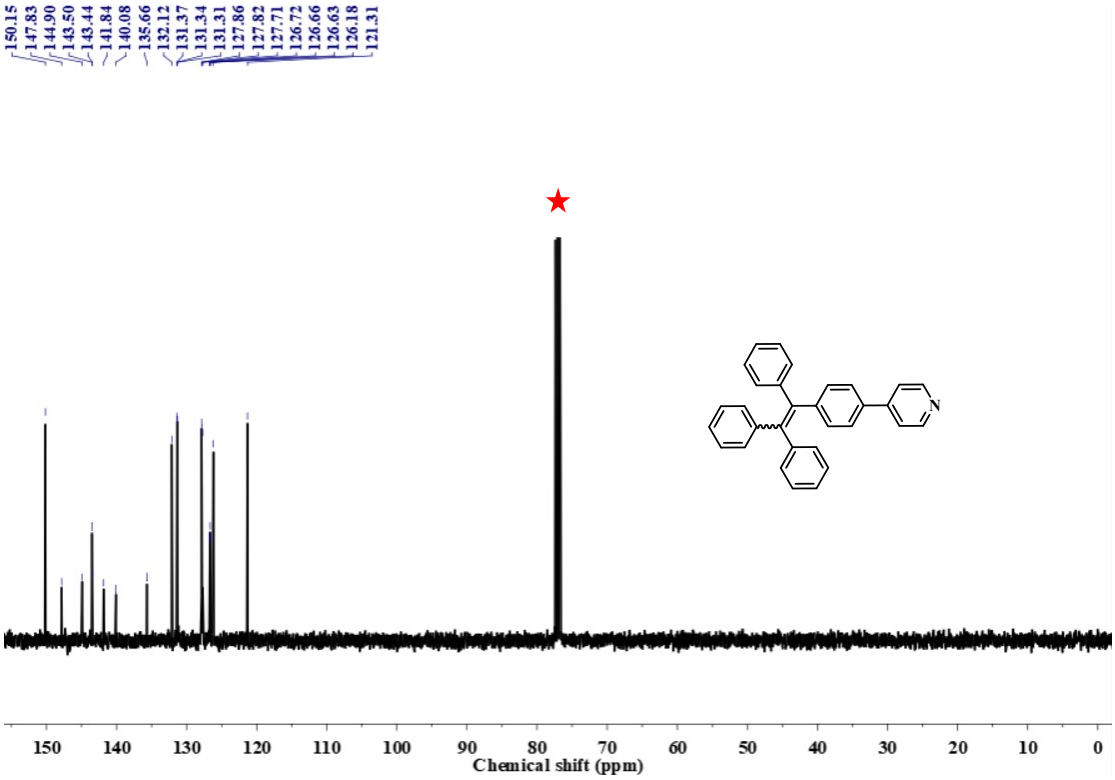

Figure S2. ^{13}C NMR Spectra of TPE-Py.

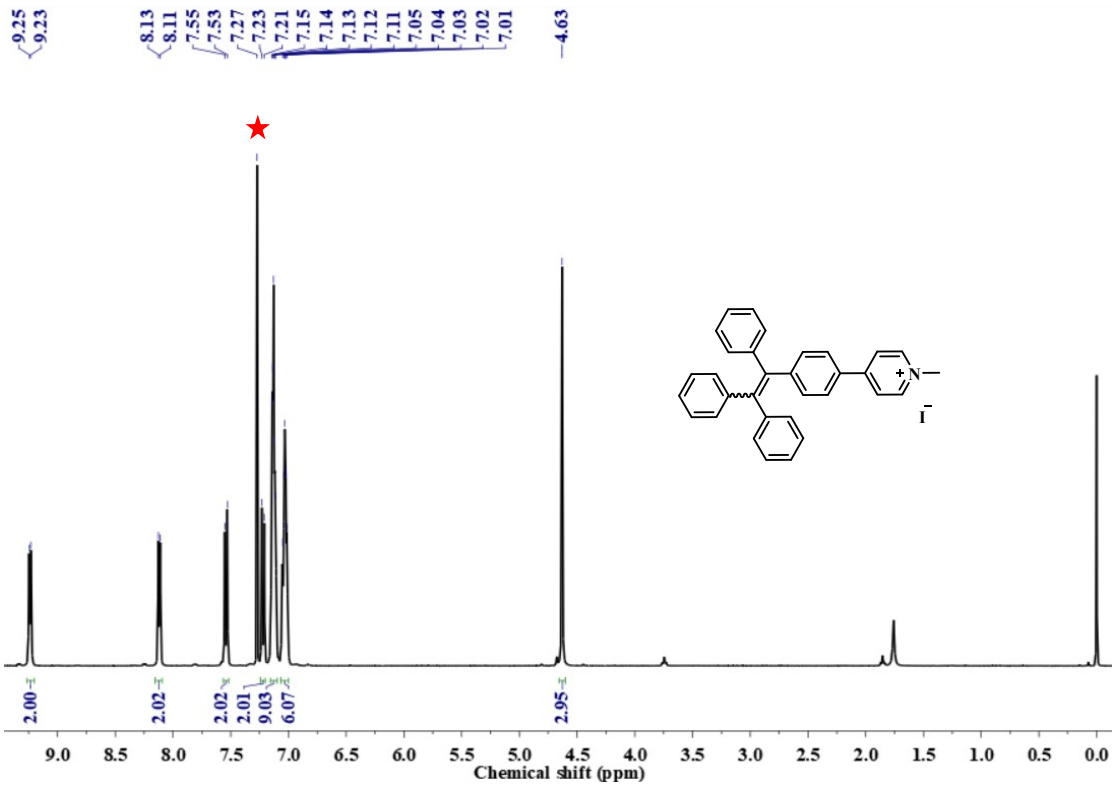

Figure S3. ^{1}H NMR Spectra of TPE-Pys-M.

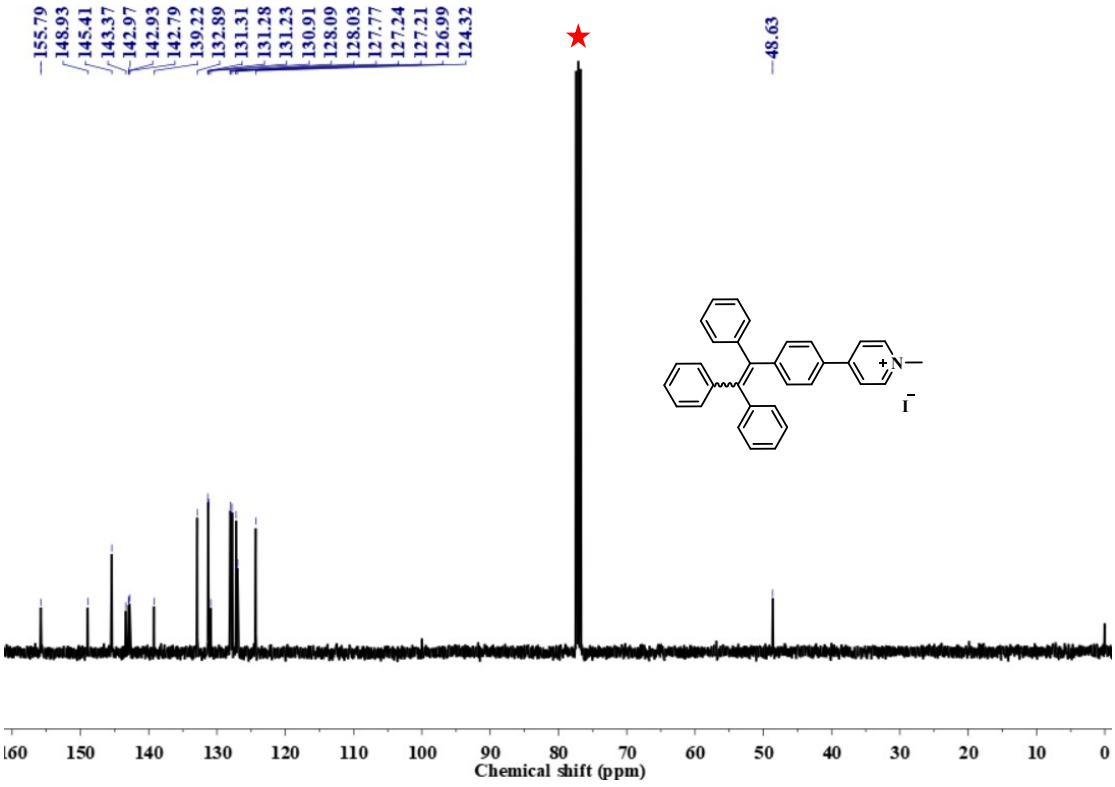

Figure S4. ^{13}C NMR Spectra of TPE-Pys-M.

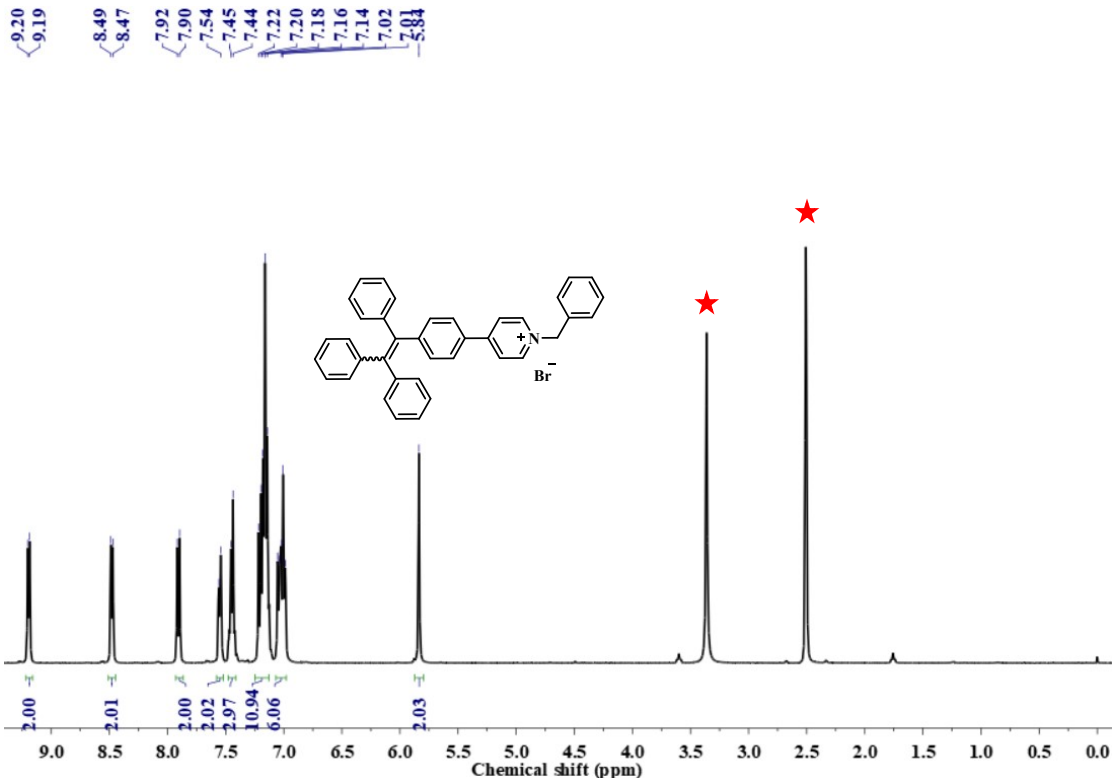

Figure S5. [1]H NMR Spectra of TPE-Pys-B.

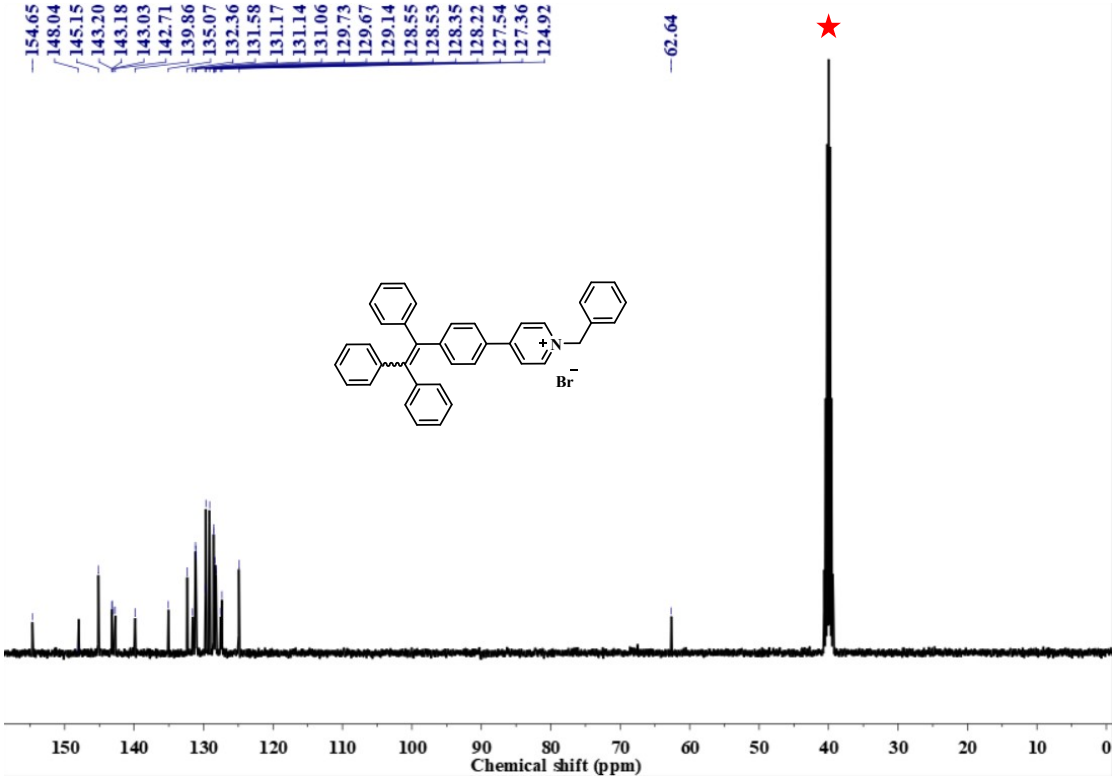

Figure S6. [13]C NMR Spectra of TPE-Pys-B.

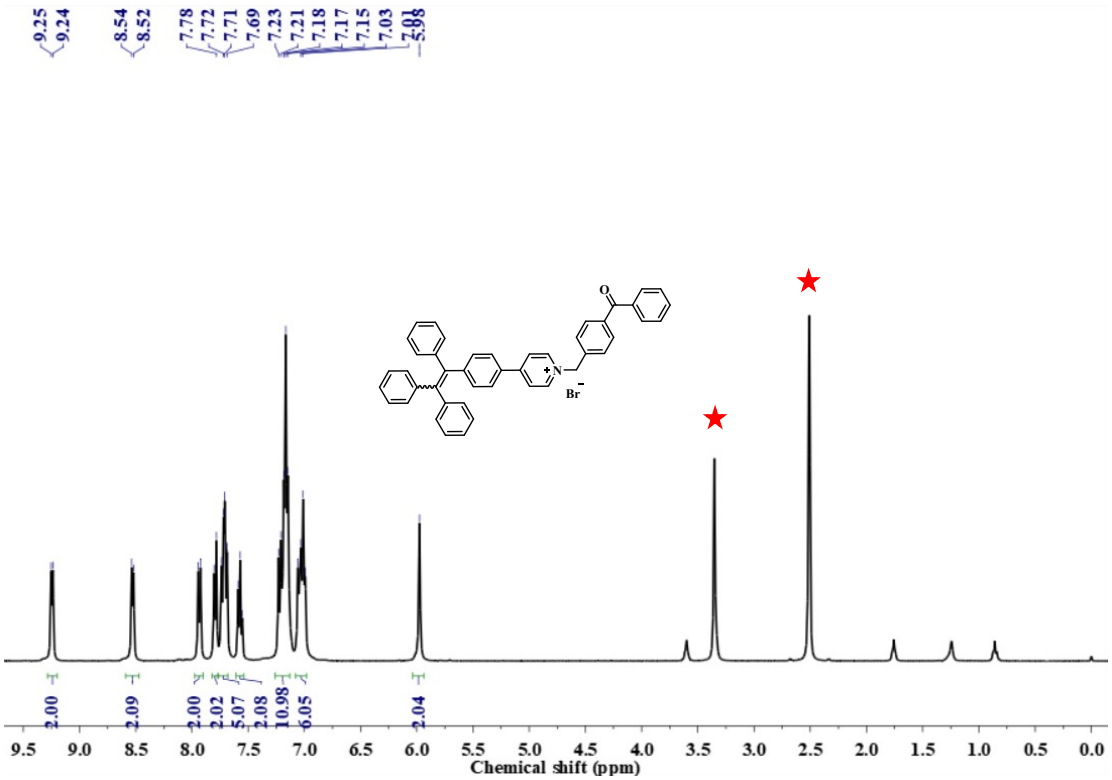

Figure S7. ^{1}H NMR Spectra of TPE-Pys-BP.

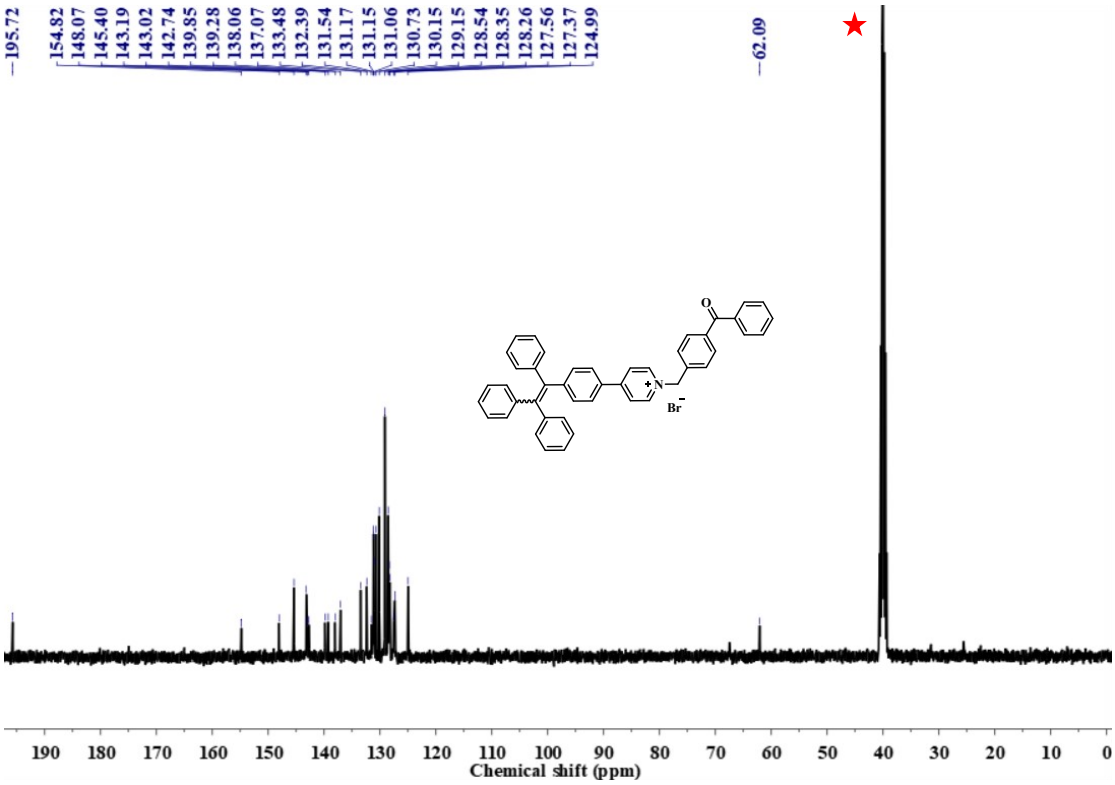

Figure S8. ^{13}C NMR Spectra of TPE-Pys-BP.

3. The date of excited state level, photophysical and photodynamic

Table S1 Calculated energy of the singlet (S) and triplet (T) excited states

Compounds	TPE-Py	TPE-Pys-M	TPE-Pys-B	TPE-Pys-BP
S_1	4.0995	2.5787	2.7070	2.6851
S_2	4.8827	3.7811	3.9276	3.7325
S_3	4.9418	3.9111	4.0600	3.9054
T_1	2.4938	1.8970	2.0066	1.9924
T_2	3.1823	2.7836	2.8155	2.8120
T_3	3.4274	3.2128	3.3068	2.9833
T_4	3.4915	3.3799	3.4062	3.2943
T_5	3.7499	3.4621	3.5109	3.3382
T_6	3.9144	3.5062	3.5626	3.4035

Table S2. Photophysical and photodynamic data of the compounds

Compounds	λ_{abs} (nm)	λ_{ex} (nm)	λ_{em} (nm) solid	Φ (%)	ε (M^{-1} cm^{-1})	τ (ns)	ROS yield (RB=1)	$\Delta E_{L\text{-}H}$ (eV)	SOC constant
TPE-Py	325	370	453	50.27	33168	2.33	0.018	3.582	0.293
TPE-Pys-M	366	452	562	13.15	39528	3.71	0.022	4.071	0.267
TPE-Pys-B	372	450	524	65.47	40291	3.57	0.024	4.232	0.272
TPE-Pys-BP	374	415	525	68.92	46830	2.63	0.818	4.209	0.446

4. Study on AIE properties of compounds

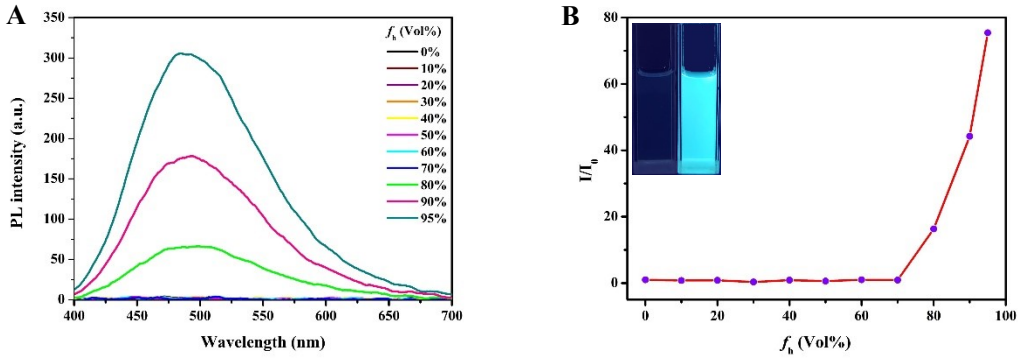

Figure S9. (A, B) PL spectra and the plot of the emission maximum of TPE-Py in dichloromethane and *n*-hexane mixture with different *n*-hexane fractions (0-95%). Inset: fluorescent photographs of TPE-Py in pure dichloromethane and in dichloromethane and *n*-hexane mixtures when the addition of *n*-hexane was 95%.

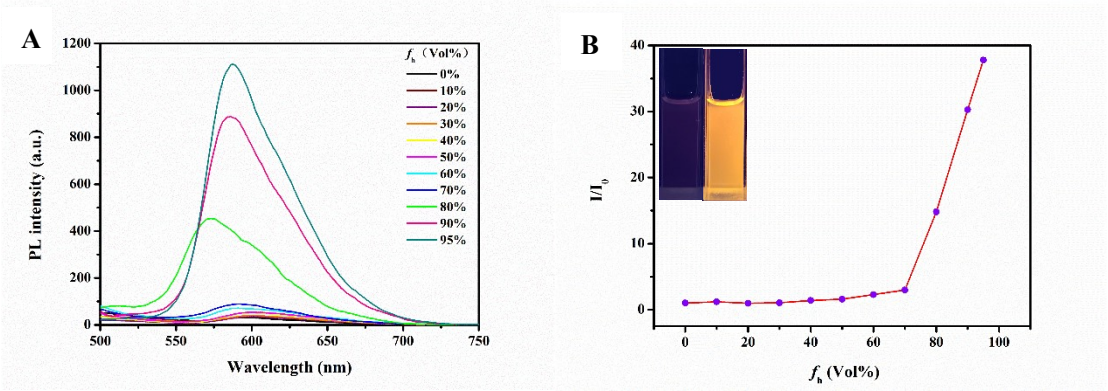

Figure S10. (A, B) PL spectra and the plot of the emission maximum of TPE-Pys-M in dichloromethane and *n*-hexane mixture with different *n*-hexane fractions (0-95%). Inset: fluorescent photographs of TPE-Pys-M in pure dichloromethane and in dichloromethane and *n*-hexane mixtures when the addition of *n*-hexane was 95%.

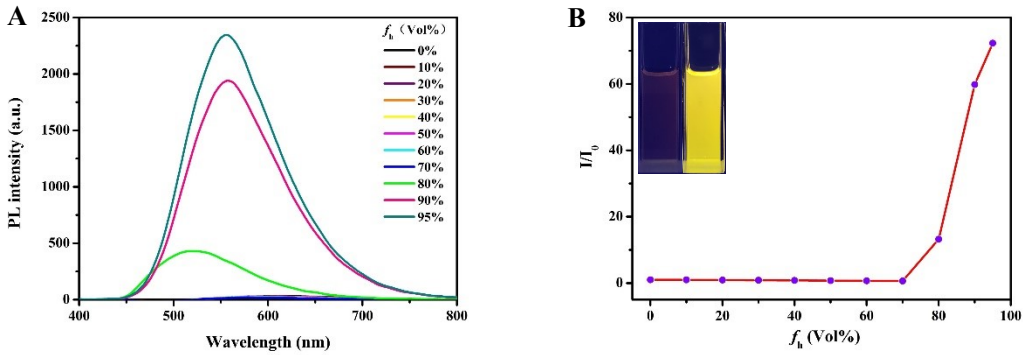

Figure S11. (A, B) PL spectra and the plot of the emission maximum of TPE-Pys-B in dichloromethane and *n*-hexane mixture with different *n*-hexane fractions (0-95%). Inset: fluorescent photographs of TPE-Pys-B in pure dichloromethane and in dichloromethane and *n*-hexane mixtures when the addition of *n*-hexane was 95%.

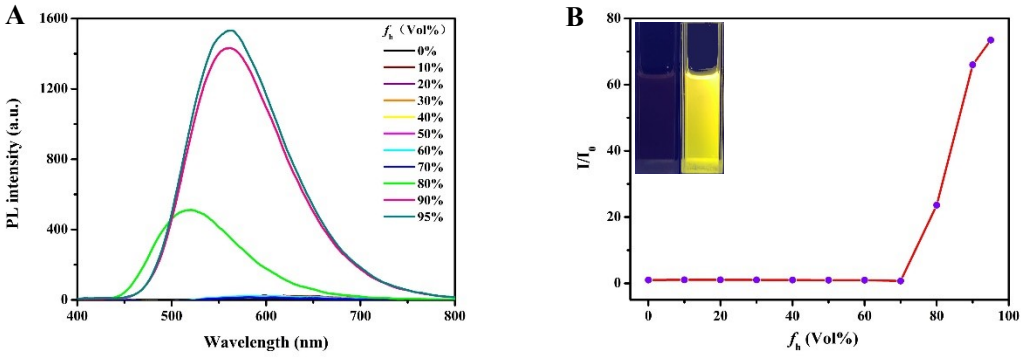

Figure S12. (A, B) PL spectra and the plot of the emission maximum of TPE-Pys-BP in dichloromethane and *n*-hexane mixture with different *n*-hexane fractions (0-95%). Inset: fluorescent photographs of TPE-Pys-BP in pure dichloromethane and in dichloromethane and *n*-hexane mixtures when the addition of *n*-hexane was 95%.

5. Photostability and solvation effect of compounds

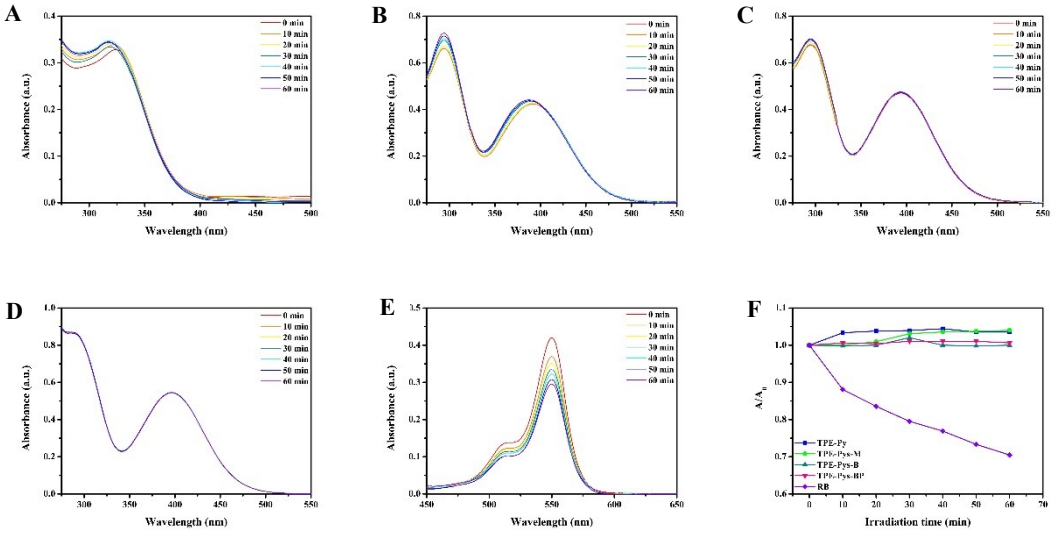

Figure S13. Photostability test of TPE-Py, TPE-Pys-M, TPE-Pys-B, TPE-Pys-BP and RB upon white light.

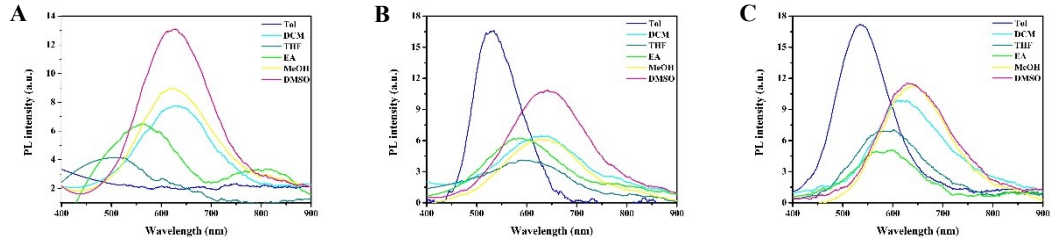

Figure S14. PL spectra of TPE-Pys-M, TPE-Pys-B and TPE-Pys-BP in different solvents.

6. Study on ROS generation of compounds

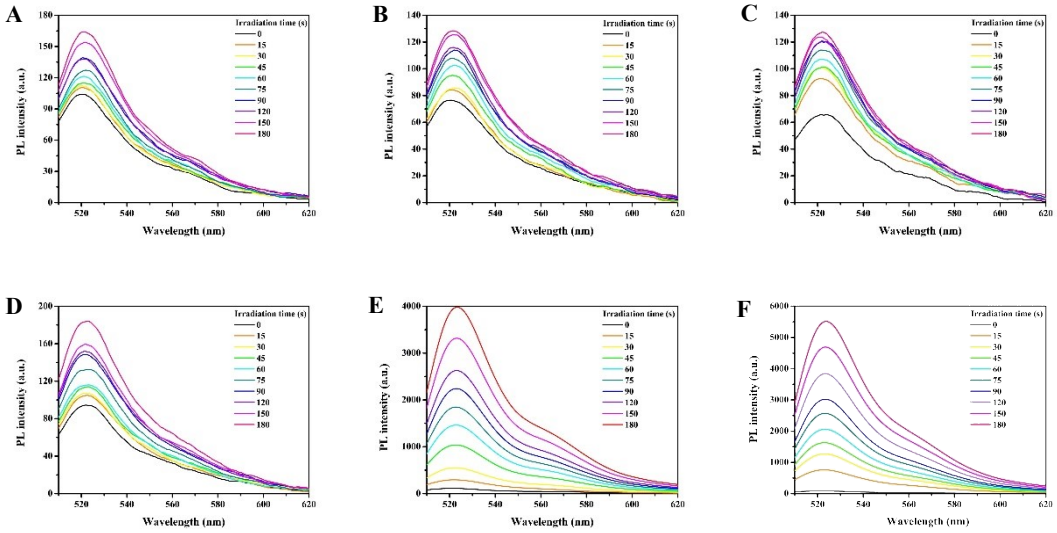

Figure S15. ROS generation of blank, TPE-Py, TPE-Pys-M, TPE-Pys-B, TPE-Pys-BP and RB (1 μM) upon exposure to white light using DCFH (10 μM) as an indicator.

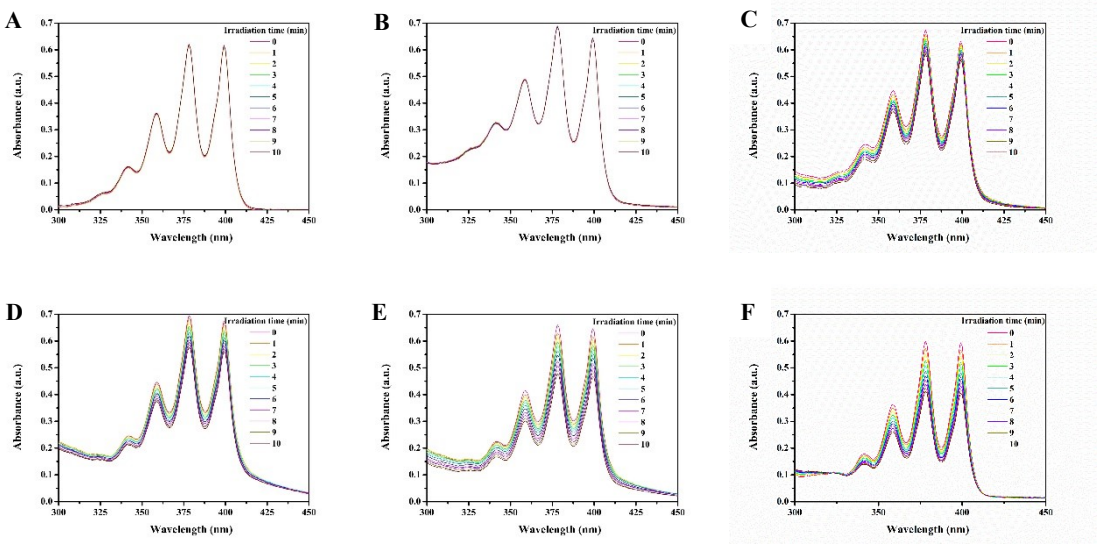

Figure S16. Absorption of ABDA (50 μM, $^1O_2$ probe) in water in the presence of blank, TPE-Py, TPE-Pys-M, TPE-Pys-B, TPE-Pys-BP and RB (10 μM) under white light irradiation for different time.

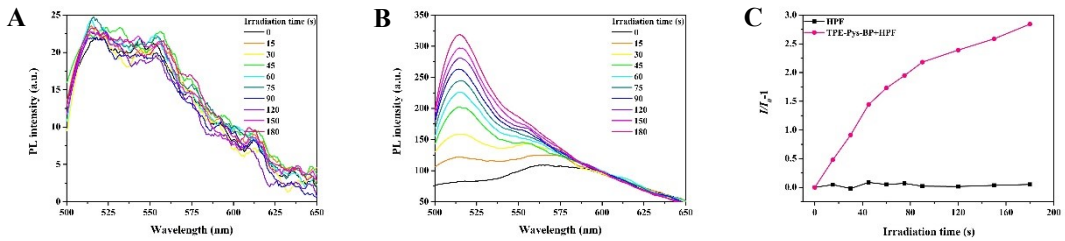

Figure S17. The PL spectra of HPF (5 μM, OH· probe) in the presence of 1 μM TPE-Pys-BP in PBS upon white light irradiation with 150 mW cm^{-2} for different times.

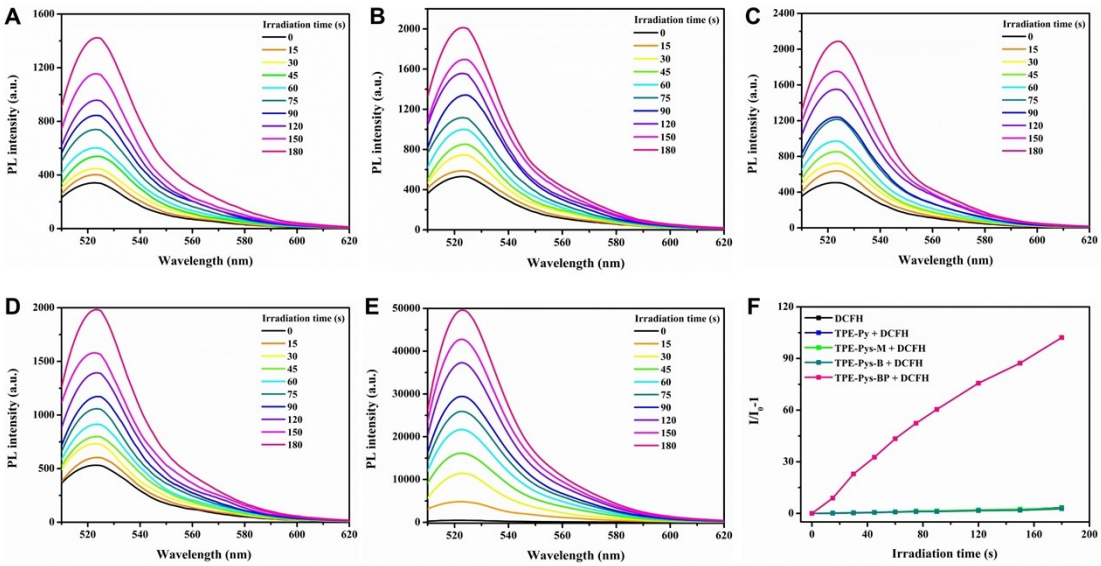

Figure S18. ROS generation of blank, TPE-Py, TPE-Pys-M, TPE-Pys-B, and TPE-Pys-BP (1 μM) upon exposure to white light (25 mW/cm^2) using DCFH (10 μM) as an indicator.

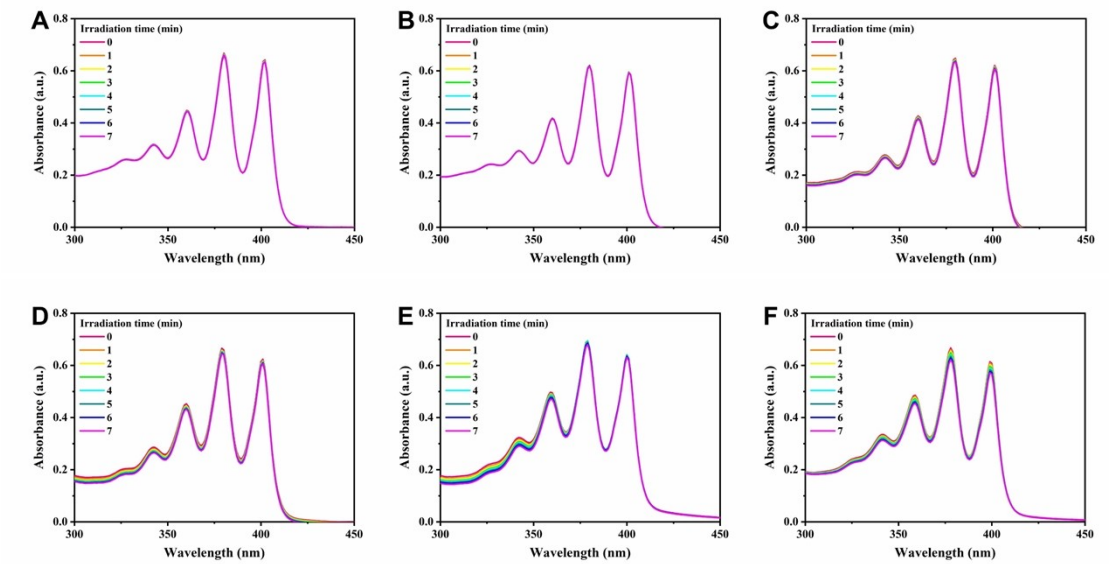

Figure S19. The absorbance spectra of ABDA (50 μM, $^1O_2$ probe) at 380 nm in the presence of TPE-Py (10 μM) in mixtures of DMSO and H_2O with different H_2O fractions (0%, 20%, 40%, 60%, 80% and 95%) upon white-light irradiation (25 W/cm^2).

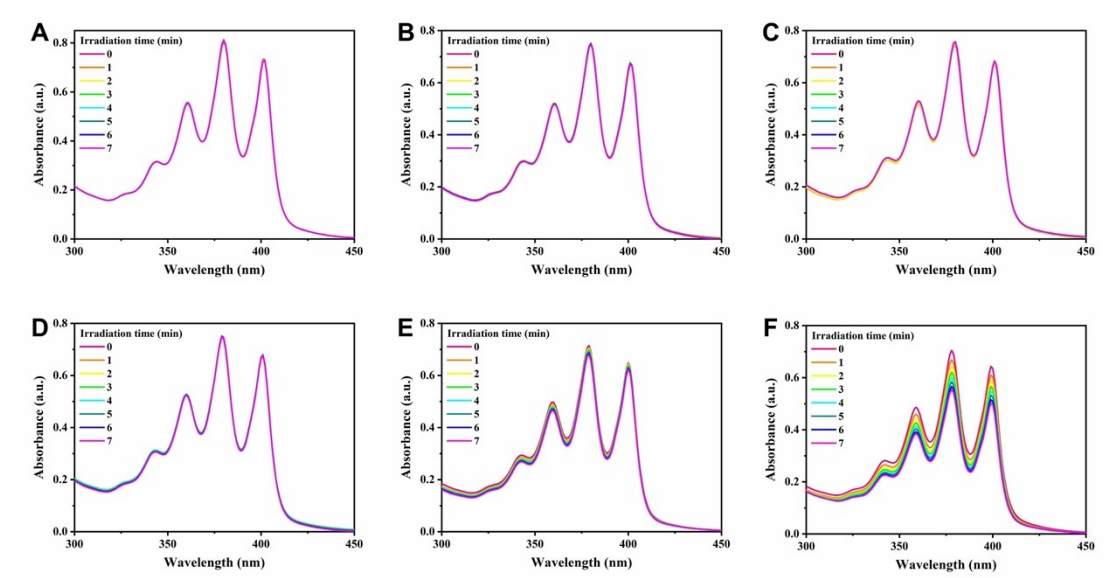

Figure S20. The absorbance spectra of ABDA (50 μM, $^1O_2$ probe) at 380 nm in the presence of TPE-Pys-M (10 μM) in mixtures of DMSO and H_2O with different H_2O fractions (0%, 20%, 40%, 60%, 80% and 95%) upon white-light irradiation (25 W/cm^2).

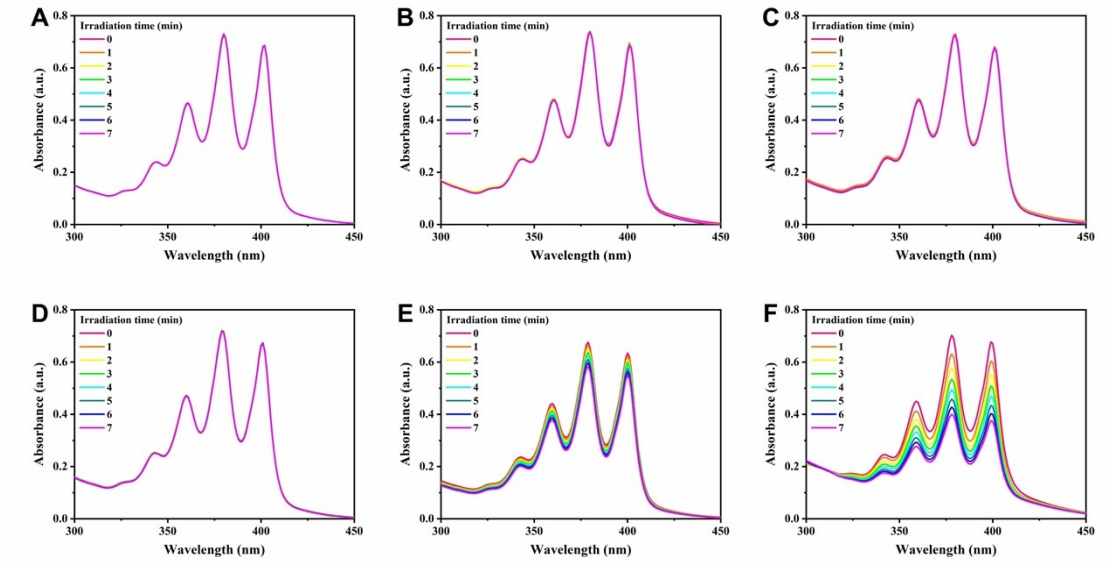

Figure S21. The absorbance spectra of ABDA (50 μM, $^1O_2$ probe) at 380 nm in the presence of TPE-Pys-B (10 μM) in mixtures of DMSO and H_2O with different H_2O fractions (0%, 20%, 40%, 60%, 80% and 95%) upon white-light irradiation (25 W/cm^2).

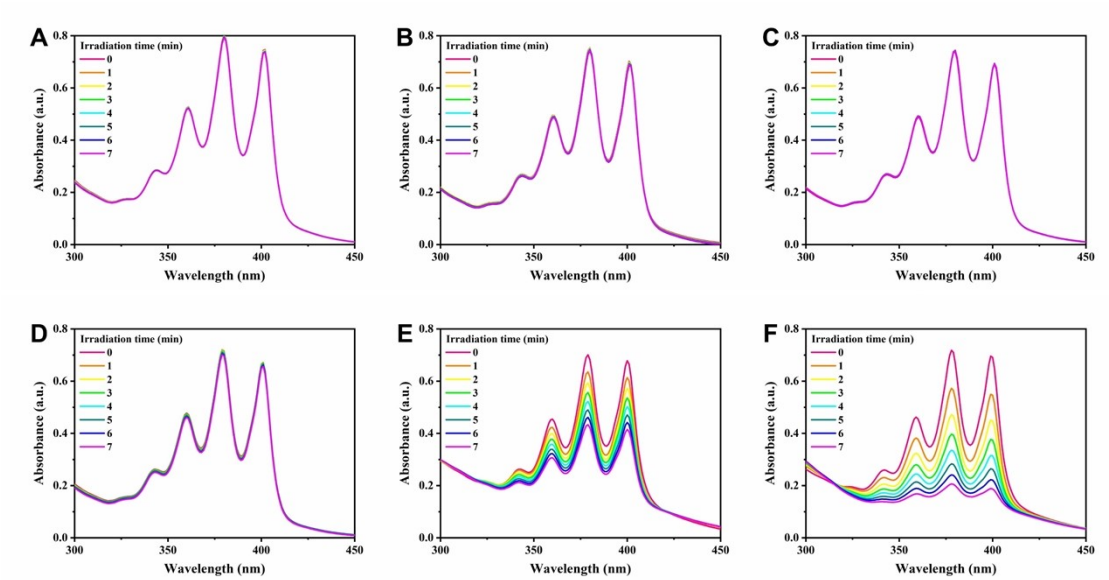

Figure S22. The absorbance spectra of ABDA (50 μM, $^1O_2$ probe) at 380 nm in the presence of TPE-Pys-BP (10 μM) in mixtures of DMSO and H_2O with different H_2O fractions (0%, 20%, 40%, 60%, 80% and 95%) upon white-light irradiation (25 W/cm^2).

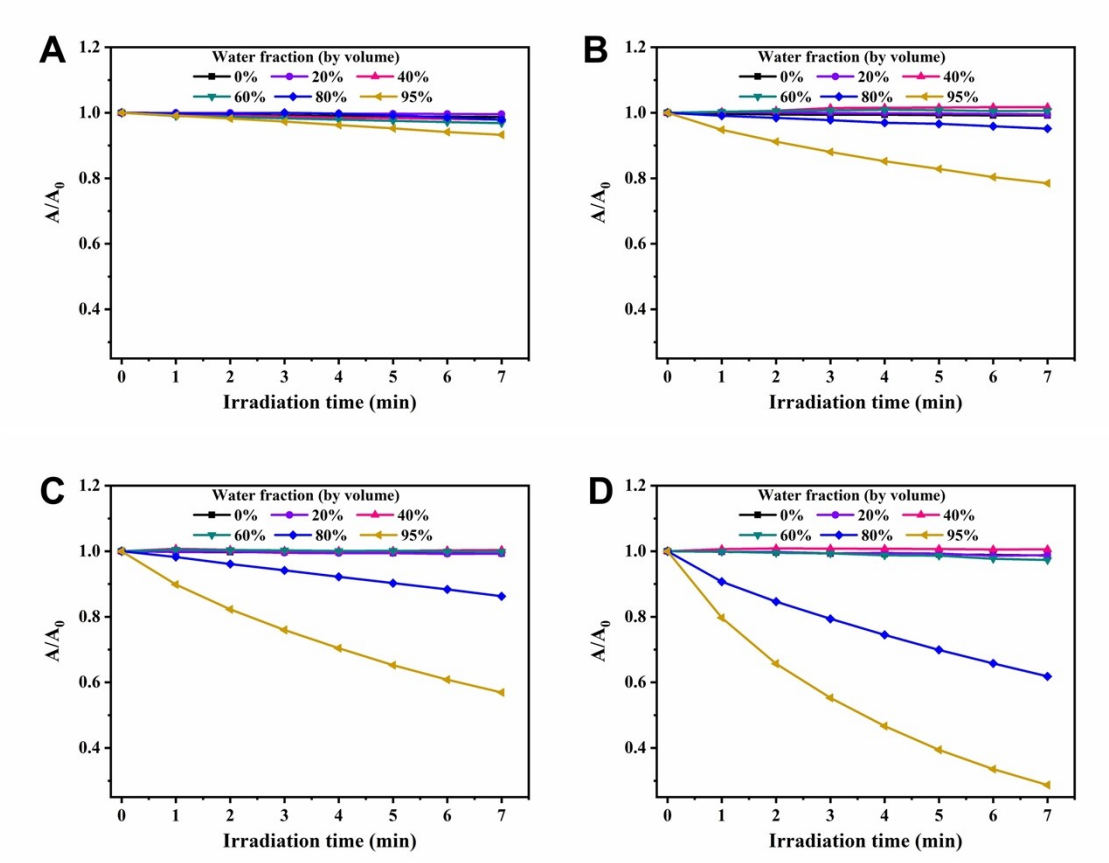

Figure S23. Photodegradation of ABDA indicative of $^1O_2$ generation induced by (A) TPE-Py, (B) TPE-Pys-M, (C) TPE-Pys-B and (D) TPE-Pys-BP respectively in DMSO/H_2O mixtures with different H_2O fractions (0%, 20%, 40%, 60%, 80% and 95%) under white light irradiation (25 mW/cm^2).

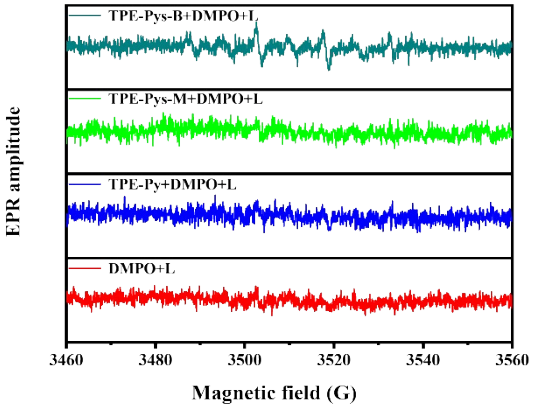

Figure S24. EPR signals of DMPO (25 mM) in the presence TPE-Py, TPE-Pys-M and TPE-Pys-B in H_2O, with/without white light irradiation (150 mW cm^{-2}) for 5 min.

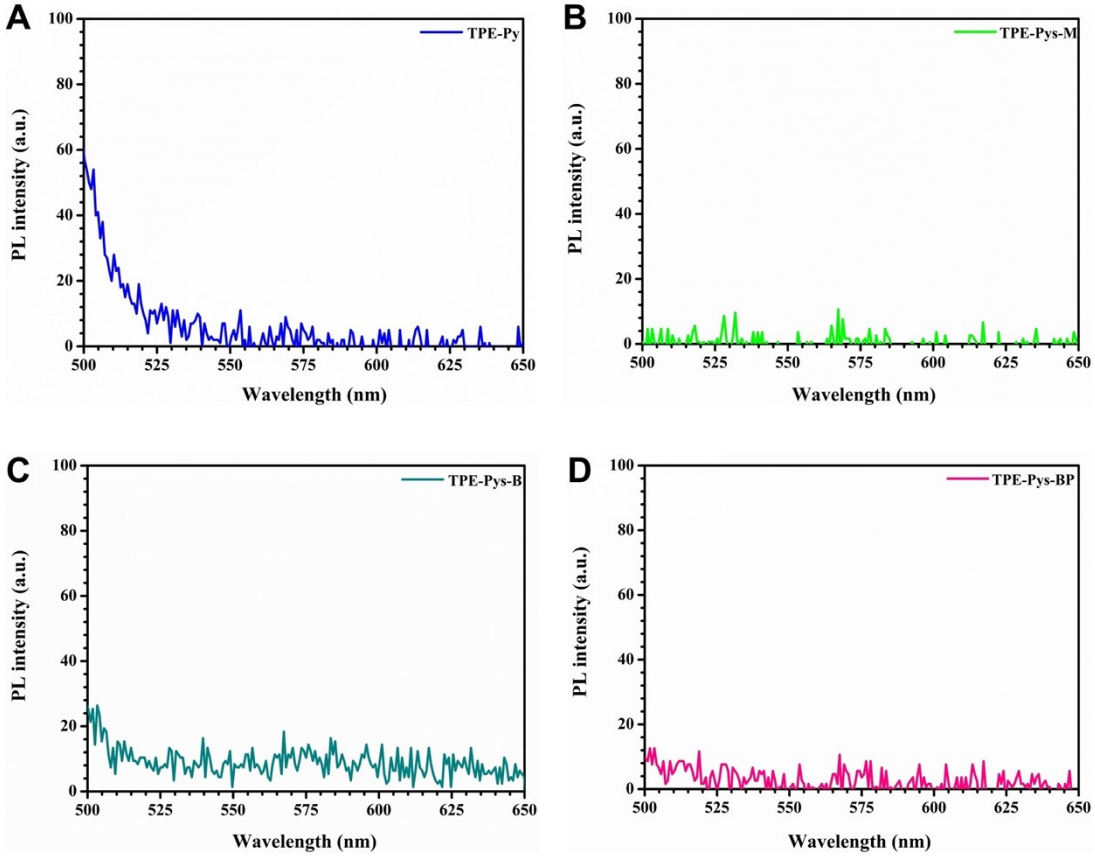

Figure. S25 PL spectra of TPE-Py, TPE-Pys-M, TPE-Pys-B and TPE-Pys-BP (conc.: 1 μM) in PBS solution (λ_{ex} = 488 nm).

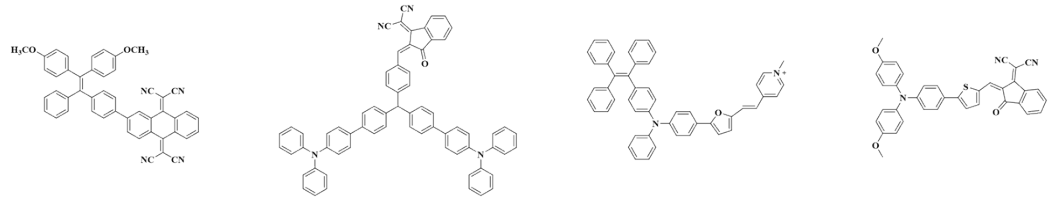

ROS yield: About 1.05-folds of RB
Adv. Mater. **2017**, *29*, 1700548

ROS yield: About 2.6-folds of RB
Biomaterials **2021**, *275*, 120934

ROS yield: About 2.2-folds of RB
Angew. Chem. Int. Ed. **2020**, *8*, 9610

ROS yield: About 1.41-folds of RB
ACS Nano **2021**, *15*, 7328

Chart 1. The ROS yield of some reported AIE photosensitizers.

7. Cell imaging and cell viability test of compounds

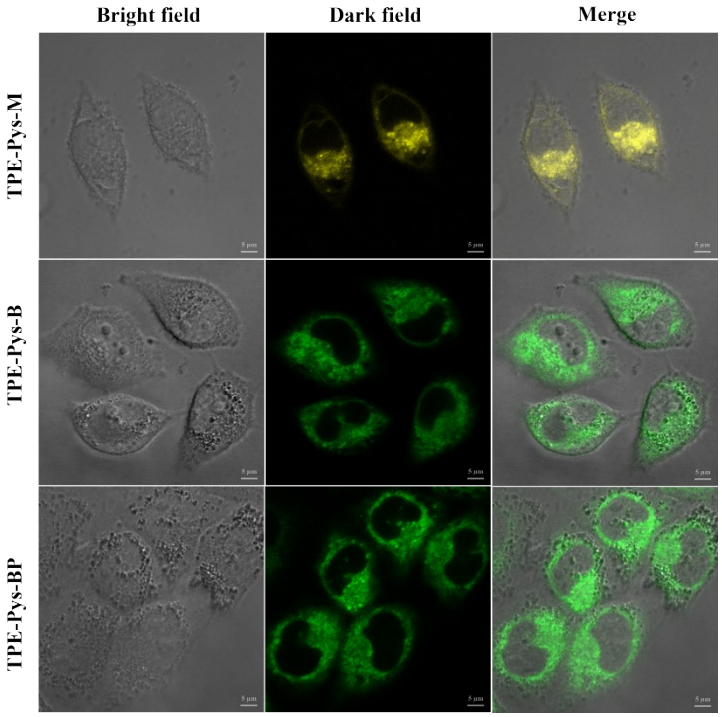

Figure S26. Fluorescence images of HeLa cells stained with 10 μM TPE-Pys-M, TPE-Pys-B and TPE-Pys-BP for 4 h respectively.

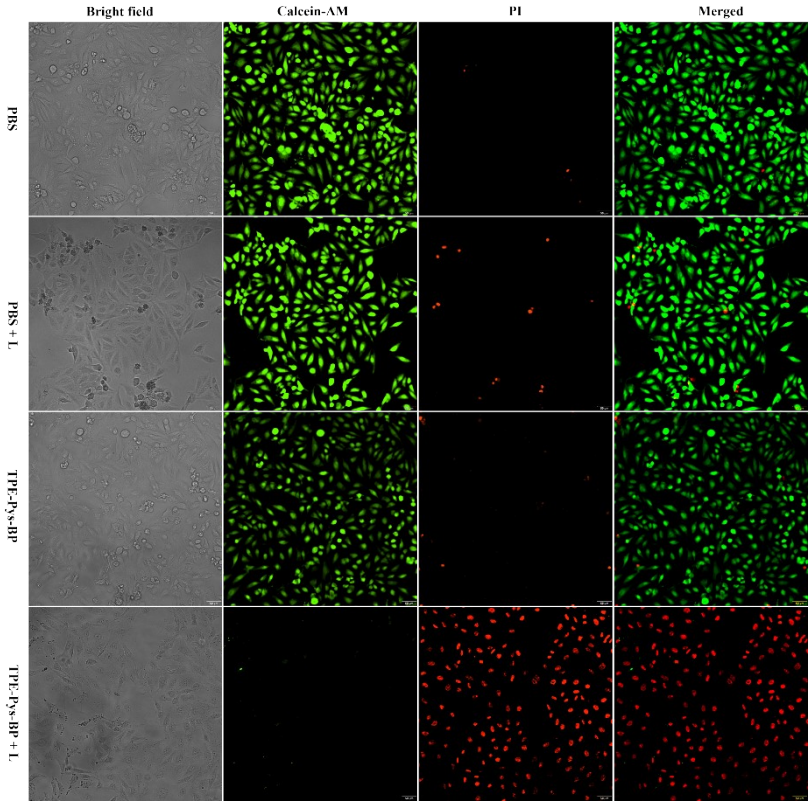

Figure S27. live/dead staining assay of Hela cells after various treatments.

8. Mechanoluminescent properties of compounds

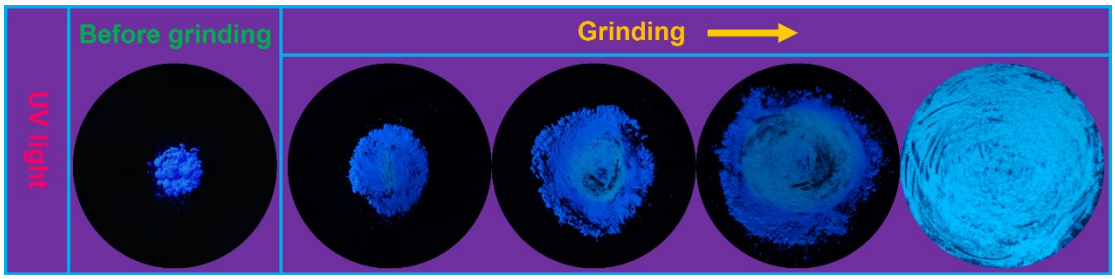

Figure S28. The photos of TPE-Py in agate mortar during grinding under illumination at 365 nm.

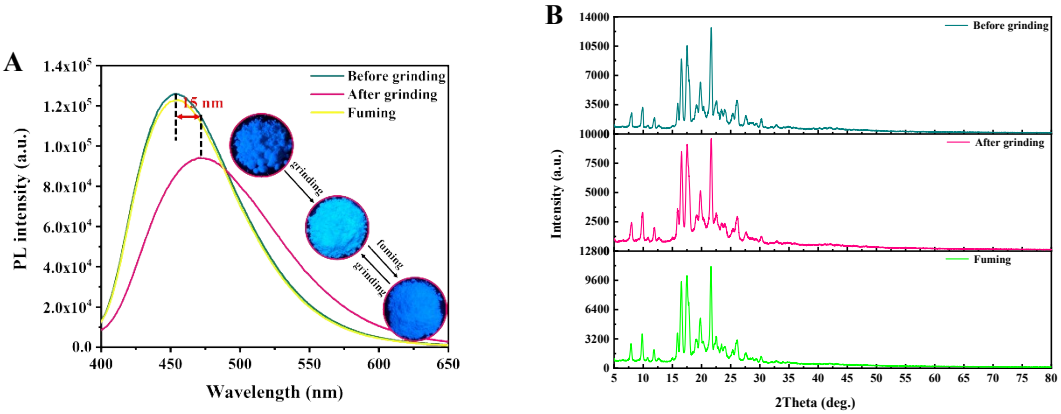

Figure S29. (A) Change in the emission spectrum of TPE-Py powder by the grinding, fuming and crystallizing process, inset: fluorescence images of TPE-Py with different treating methods. (B) X-ray diffraction (XRD) spectra of TPE-Py in different aggregated states.

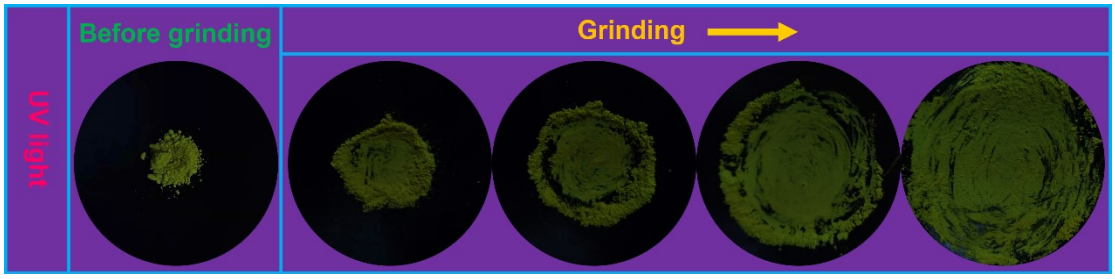

Figure S30. The photos of TPE-Pys-M in agate mortar during grinding under illumination at 365 nm.

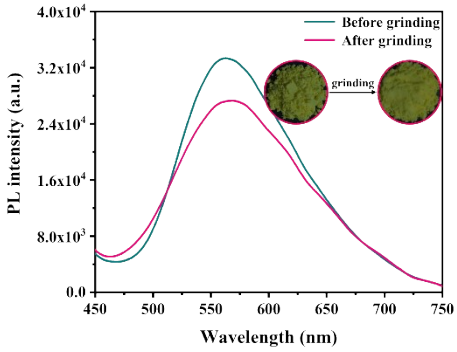

Figure S31. Changes of emission spectra of TPE-Pys-M before and after grinding.

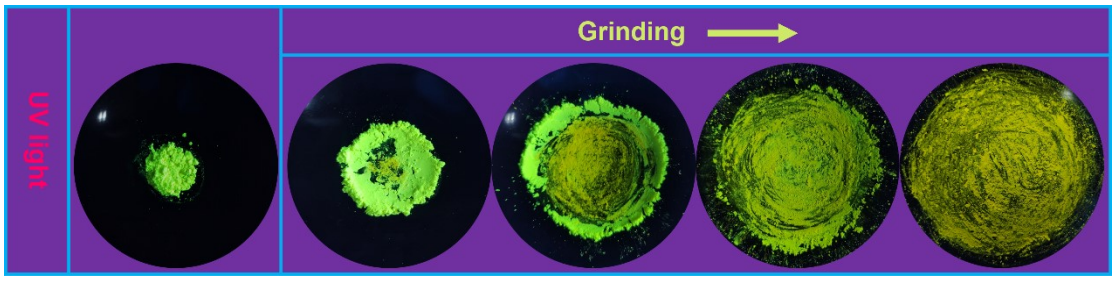

Figure S32. The photos of TPE-Pys-B in agate mortar during grinding under illumination at 365 nm.

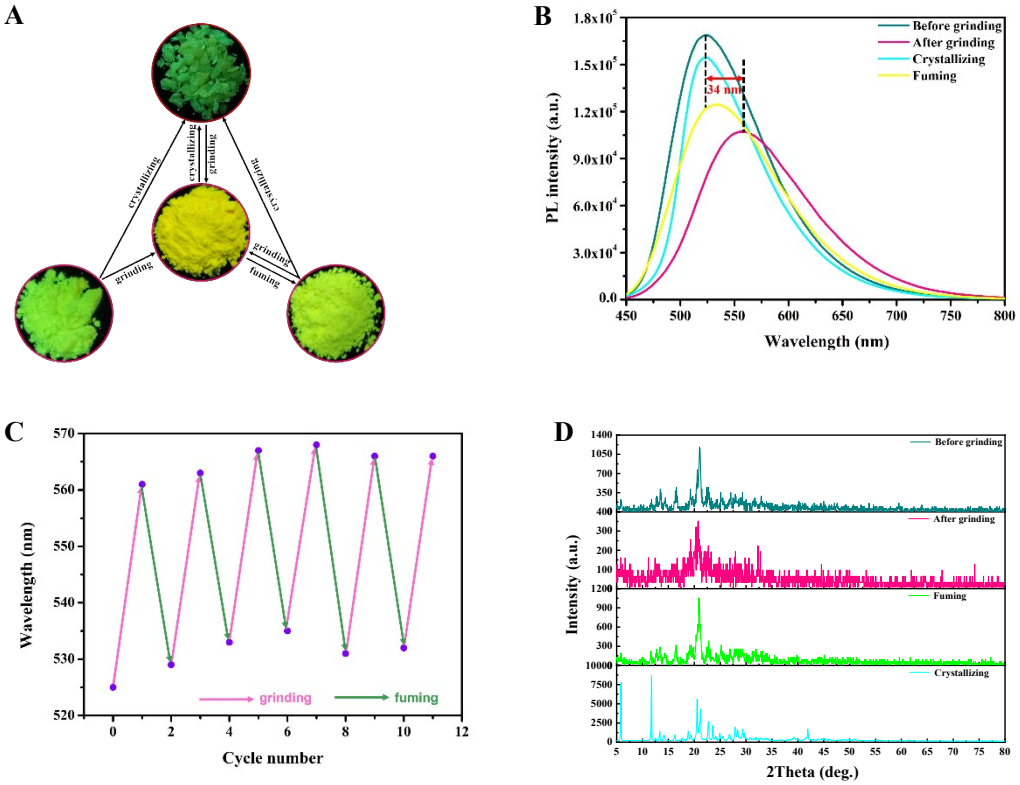

Figure S33. (A) Reversible mechanochromic fluorescence images of TPE-Pys-B with different treating methods. (B)Change in the emission spectrum of TPE-Pys-B powder by the grinding, fuming and crystallizing process. (C) X-ray diffraction (XRD) spectra of TPE-Pys-B in different aggregated states. (D) Repeated switching of the solid-state fluorescence of TPE-Pys-B by repeated grinding and fuming cycles.

9. Single crystal date of TPE-Pys-B

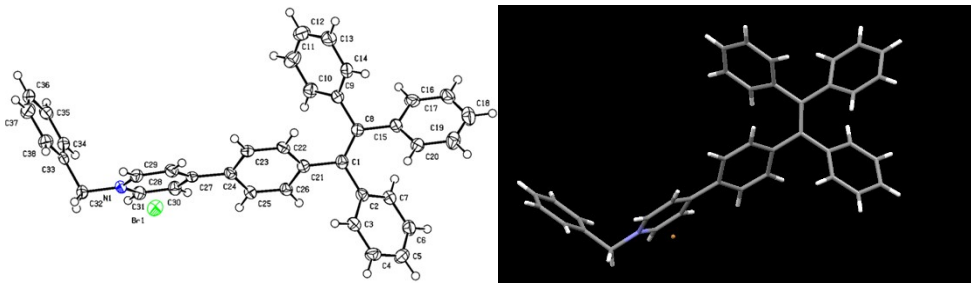

Figure S34. Single crystal structure of TPE-Pys-B.

Table S3. Crystal data and structure refinement for TPE-Pys-B.

Identification code	TPE-Pys-B
Empirical formula	$C_{38}H_{30}BrN$
Formula weight	580.54
Temperature/K	150.00(10)
Crystal system	monoclinic
Space group	$P2_1$
a/Å	9.1911(2)
b/Å	10.7975(2)
c/Å	15.0783(3)
α/°	90
β/°	97.991(2)
γ/°	90
Volume/Å^3	1481.85(5)
Z	2
ρ_{calc}g/cm^3	1.301
μ/mm^{-1}	2.080
F(000)	600.0
Crystal size/mm^3	0.14 × 0.12 × 0.11
Radiation	Cu Kα (λ = 1.54184)
2Θ range for data collection/°	5.918 to 133.12
Index ranges	$-10 \le h \le 10$, $-12 \le k \le 11$, $-17 \le l \le 17$
Reflections collected	8600
Independent reflections	4060 [R_{int} = 0.0199, R_{sigma} = 0.0241]
Data/restraints/parameters	4060/1/361
Goodness-of-fit on F^2	1.026
Final R indexes [I>=2σ (I)]	R_1 = 0.0343, wR_2 = 0.0937
Final R indexes [all data]	R_1 = 0.0345, wR_2 = 0.0939
Largest diff. peak/hole / e Å^{-3}	0.60/-0.39
Flack parameter	0.018(19)